

Contribution of on-site Coulomb repulsion energy to structural, electronic and magnetic properties of SrCoO₃ for different space groups: first-principles study

SHIBGHATULLAH MUHAMMADY*, INGE M. SUTJAHJA

Department of Physics, Faculty of Mathematics and Natural Sciences, Institut Teknologi Bandung, Ganesha 10, Bandung 40132, Indonesia

We report structural, electronic, and magnetic properties of SrCoO₃ in Pm $\bar{3}$ m and P4/mbm space groups, which are calculated by using generalized gradient approximation corrected with on-site Coulomb repulsion U and exchange energies J. The cubic lattice parameter a and local magnetic moments of Co (μ_{Co}) are optimized by varying U at Co 3d site. Employing ultrasoft pseudopotential, the values of U = 8 eV and J = 0.75 eV are the best choice for Pm $\bar{3}$ m space group. We found the value of $\mu_{\text{Co}} = 2.56 \mu_{\text{B}}$, which is consistent with the previous results. It was also found that Co 3d, hybridized with O 2p, is the main contributor to ferromagnetic metallic properties. Besides, norm-conserving pseudopotential promotes a, which is in good agreement with experimental result. However, it is not suitable for P4/mbm space group. By using ultrasoft pseudopotential, the value of U = 3 eV (J = 0.75) is the most suitable for P4/mbm group. Ferromagnetic metallic properties, Jahn-Teller distortion, and reasonable lattice parameters have been obtained. This study shows that U has significant contribution to the calculated properties and also points out that P4/mbm space group with US-PP is suitable to describe experimental results.

Keywords: *structural properties; electronic properties; magnetic properties; SrCoO₃; on-site Coulomb repulsion energy*

1. Introduction

The oxide perovskite ABO₃ (A is the cation with larger size than that of B) of transition metal element has become an interesting system due to its diverse and rich physical properties, ranging from ferroelectric (SrTiO₃) [1], ferromagnetic (FM) (SrCoO₃) [2], giant magnetoelectric (SrMnO₃ and SmFeO₃) [3, 4]. In particular, for cobalt oxide materials, the valence state of Co ions strongly depends on the type and concentration of dopant, leading to non-stoichiometric value of oxygen content and variation in the valence state of Co²⁺ (3d⁷), Co³⁺ (3d⁶), Co⁴⁺ (3d⁵) or fractional valence state as well as mixed valence states. Under crystal field potential with a certain symmetry from the surrounding oxygen ligand, the 5 degenerate d-orbitals split into 3-fold degenerated t_{2g} and 2-fold degenerated e_g orbitals. Furthermore, the proximity of crystal-field splitting energy (Δ_{cf}) of

t_{2g} – e_g and Hund rule intra-atomic exchange energy J result in the variation of Co spin state, namely low-spin (LS) state (t_{2g}⁶e_g⁰, S = 0), intermediate-spin (IS) state (t_{2g}⁵e_g¹, S = 1) or the high-spin (HS) state (t_{2g}⁶e_g², S = 2). All of these matters are responsible for more susceptible properties of cobalt oxide system as observed with the emergence of metal-insulator [5] and spin-state transitions [6] toward the external effects, such as temperature, pressure, or magnetic field.

In particular, perovskite cobalt oxide of SrCoO_{3- δ} is very interesting, since it can be used as a cathode material of solid oxide fuel cells [7] and active material in spintronic devices [8]. It has also been found that the structural and magnetic properties of SrCoO_{3- δ} sensitively depend on O₂ and applied pressure. The stoichiometric SrCoO₃ that crystallizes in Pm $\bar{3}$ m space group [9] can be obtained from orthorhombic brownmillerite SrCoO_{2.5} with Pnma space group [10], at O₂ pressure and temperature of 6.5 GPa and 1023 K, respectively. Conversely, it has also been shown that

*E-mail: mshibghatullah@gmail.com

SrCoO₃ can be transformed into SrCoO_{2.5} in H₂ atmosphere by using the reduction process. Interestingly, the oxidation process provokes semi-reversible transformation of SrCoO_{2.5} back into SrCoO₃ [11]. The previous experimental results [9] showed that SrCoO₃ is FM metallic with relatively high Currie temperature of about 305 K for $\delta = 0$. The most probable spin state, which is influenced by Δ_{cf} and J, is IS-state for Co⁴⁺ ion based on the saturation magnetic moment of 2.5 μ_B /f.u. at 7 K.

Regarding first-principles studies, suitable on-site Coulomb repulsion energy U, or so called Hubbard energy, and J, exchange energy, at Co 3d site are required to obtain an accurate description of SrCoO₃. Although the electronic-structure calculation of SrCoO₃ has shown the FM metallic properties of the compound [12], the values of U and J still vary significantly for different methods, as summarized in Table 1 for Pm $\bar{3}$ m and P4/mbm space groups. P4/mbm space group has been used by rotating SrCoO₃ primitive cell by the angle of 45° leading to $\sqrt{2} \times \sqrt{2} \times 1$ supercell [2].

In this paper, we report a first-principles study on the structural, electronic, and magnetic properties of perovskite SrCoO₃ for Pm $\bar{3}$ m and P4/mbm space groups based on density-functional theory (DFT). Hohenberg-Kohn and Kohn-Sham scheme-based DFT [28, 29] have been used to calculate the properties of molecules [20–22] and solids [10, 14, 23–25]. The calculation in present study is performed by means of generalized gradient approximation (GGA) method, which has some advantages compared with local density approximation (LDA) in terms of better description of molecules and solids [26]. Besides, the magnetic and electrical properties obtained from spin-polarized projected density of states (PDOS), corresponding lattice parameters and local magnetic moment of Co ion (μ_{Co}) are also used to determine suitable values of U and J. The results are then compared with previous experimental and calculation results. The analysis is performed in three main frameworks. The first and second frameworks concern Pm $\bar{3}$ m and P4/mbm space groups, respectively. The third framework reveals the properties using norm-conserving pseudopotential (NC-PP),

compared with that calculated using ultrasoft pseudopotential (US-PP). Hence, this study elucidates not only the suitable values of U and J for SrCoO₃ in different space groups but also the employed PP.

2. Computational

A plane-waves-based Quantum ESPRESSO package [27] was used to perform spin-polarized density-functional calculation [28, 29]. The generalized gradient approximation (GGA) method was used alongside the Perdew-Burke-Ernzerhof exchange-correlation (XC) functional type [26]. The calculation was performed using Broyden mixing which employes quasi-Newton method [30]. The first calculation was performed to obtain electronic structures of 5-atom SrCoO₃ unit cell within Pm $\bar{3}$ m space group as the first model. The initial cubic lattice parameter a of 3.8289 Å based on the previous experimental result [9] and a k-point mesh of 8 × 8 × 8 centered at Γ high-symmetry k-point, were employed. The SrCoO₃ supercell is shown in Fig. 1. A kinetic energy cutoff of 25 Hartree (~680 eV) was used. Rappe-Rabe-Kaxiras (RRK) and Vanderbilt scheme-based US-PP [31, 32] were used for all atoms of the first model. The cubic lattice parameters and all atomic positions were optimized by Broyden-Fletcher-Goldfarb-Shanno-minimization (BFGS) algorithm [33–36]. Besides, the nonlinear core [37] and/or semi-core correction [38] were employed for obtaining reliable description of US-PP. For realizing a Hubbard model, the cubic lattice parameter and local magnetic moments of Co (μ_{Co}) and O (μ_O) ions were optimized as function of effective Hubbard potential energy values of $U_{eff} = U - J$. The Hubbard model (for GGA method) is described as [39]:

$$E_{GGA+U} [n] = E_{GGA} [n] + E_U [\{n_{mm'}^{i\sigma}\}] \quad (1)$$

$$E_U [\{n_{mm'}^{i\sigma}\}] = E_{Hub} [\{n_m^{i\sigma}\}] - E_{DC} [\{n^{i\sigma}\}] \quad (2)$$

where $n(r)$ is the electron density at position r , $n_m^{i\sigma}$ is the spin-polarized occupation of atomic-orbital for the atom i on which the Hubbard is applied, and $n^{i\sigma}$ is expressed as:

$$n^{i\sigma} = \sum_m n_m^{i\sigma} \quad (3)$$

Table 1. Summary of previously reported results for SrCoO₃.

Space group	U [eV]	J [eV]	U _{eff} [eV]	Literature	Method	Electronic and magnetic properties
Pm $\bar{3}$ m	10.83	0.76	10.07	[13]	LDA and DMFT ^a	FM metallic
Pm $\bar{3}$ m	7.0	0.65	6.35	[10]	LDA	FM metallic
Pm $\bar{3}$ m	8.0	–	–	[14]	GGA + U	FM metallic
Pm $\bar{3}$ m	2.5	1.0	1.5	[5]	GGA + U	FM metallic
Pm $\bar{3}$ m	–	–	2.75	[15]	GGA + U and GF ^b	FM metallic
Pm $\bar{3}$ m	5.0	0.84	4.16	[16]	UHF ^c	FM half-metallic
Pm $\bar{3}$ m, P4/mbm	6.0	–	6.0	[2]	GGA + U	FM metallic

^aDynamical mean-field theory [17].

^bGreen function [18].

^cUnrestricted Hartree-Fock [19].

The term of E_{DC} is the double-counting term introduced to avoid double counting in E_{GGA} and E_{Hub} terms. The term E_U is the corresponding Hubbard term in the GGA + U method, which can be further expressed as [39, 40]:

$$E_U[\{n_{mm'}^{i\sigma}\}] = \frac{1}{2} \sum_{m,m',\sigma} U (n_m^{i\sigma} - n^0) (n_{m'}^{i-\sigma} - n^0) + \frac{1}{2} \sum_{\substack{m,m',\sigma \\ (m \neq m')}} U_{\text{eff}} (n_m^{i\sigma} - n^0) (n_{m'}^{i\sigma} - n^0) \quad (4)$$

In this study, we have introduced various values of U and J, each of them in a range of 0 eV to 10 eV and 0.60 eV to 0.75 eV, respectively.

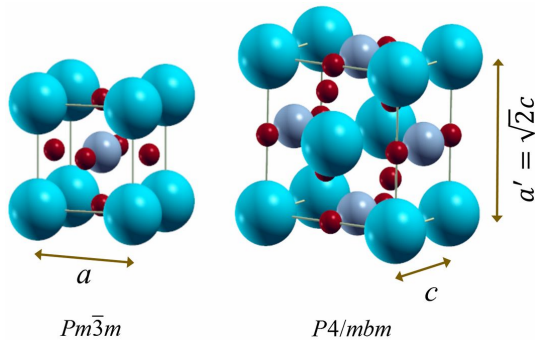


Fig. 1. Schematic diagram of SrCoO₃ in Pm $\bar{3}$ m and P4/mbm space groups. Grey, green, and red colors denote Co, Sr, and O atoms, respectively.

The second model is a 10-atom $\sqrt{2} \times \sqrt{2} \times 1$ SrCoO₃ supercell with P4/mbm space group.

Initial tetragonal lattice parameters used for the supercell are $c = 3.8289 \text{ \AA}$, based on experimental report [9], and $a' = \sqrt{2}c = 5.414882309 \text{ \AA}$. The SrCoO₃ supercell is shown in Fig. 1. To avoid time-consuming calculation, we reduced the corresponding k-point mesh to $4 \times 4 \times 6$, which is also centered at Γ high-symmetry k-point. A reduced kinetic energy cutoff of 20 Hartree ($\sim 544 \text{ eV}$) was used. The structure was also optimized using BFGS scheme and US-PP is also used for this calculation. We changed U of 0 eV to 10 eV while J was set to be 0.75 eV. The reason of the using of the values of U and J will be discussed later. Our results obtained by using US-PP have been compared with those obtained by using norm-conserving pseudopotential (NC-PP) based on Troullier-Martins scheme [41–43].

3. Results and discussion

3.1. Bulk SrCoO₃ in Pm $\bar{3}$ m space group

The calculated cubic lattice parameter and its dependence on U for some values of J, i.e. $J = 0.60 \text{ eV}$, 0.65 eV , 0.70 eV and 0.75 eV , are shown in Fig. 2. The lattice parameter a is not significantly affected by the J value, and it increases linearly with increasing of U. Unfortunately, the value of $a = 4.08 \text{ \AA}$ for $U = 10 \text{ eV}$ is overestimated. The previous report presented U and J dependences of a for $U = 0.0 \text{ eV}$, 6.5 eV , 7.0 eV , 7.5 eV and $J = 0.00 \text{ eV}$, 0.60 eV , 0.65 eV ,

0.70 eV. The resulted a values were in the range from 3.71 Å ($U = 0, J = 0$) to 3.92 Å ($U = 6.5, J = 0.60$) [10]. It is thus concluded that the calculated a for $U < 10$ eV is in a good agreement with the previously reported a, estimated experimentally and theoretically, as summarized in Table 2 and Table 3, respectively. The calculated value of a for $U < 10$ eV is close to that of the theoretically calculated by using LDA + U and GGA + U and also to the experimental a for small U. However, a calculated using hybrid calculation gives the overestimated value [2].

The analysis of U and J is then extended by using the calculated local magnetic moments of Co ions (μ_{Co}). As it is shown in Fig. 3, μ_{Co} increases linearly with increasing of U for $U \leq 6$ eV and jumps up for $U = 7$ eV. For $7 \text{ eV} < U < 9 \text{ eV}$, μ_{Co} does not change and jumps up for $9 \text{ eV} < U \leq 10 \text{ eV}$. The U-dependent behavior of μ_{Co} is consistent with that of previous report, in which μ_{Co} linearly increased until $U = 7$ eV and saturated for $7 \text{ eV} < U < 9 \text{ eV}$ [14]. Furthermore, the values of U of 8 eV and 9 eV, $J = 0.75$ eV provide very similar μ_{Co} values of $2.56 \mu_{\text{B}}$ and $2.57 \mu_{\text{B}}$, which are in good agreement with the previous theoretical result of $3.19 \mu_{\text{B}}$ ($U = 8.0 \text{ eV}$) [14] and experimental result of 3.0 eV [44].

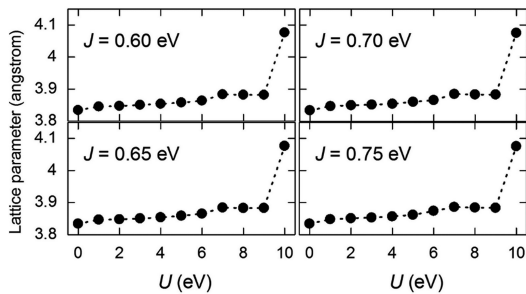


Fig. 2. Calculated cubic lattice parameter of SrCoO_3 as function of U for selected values of J from $J = 0.60 \text{ eV}$ to 0.75 eV in $\text{Pm}\bar{3}\text{m}$ space group.

The value of $\mu_{\text{Co}} = 2.56 \mu_{\text{B}}$ or $\mu_{\text{Co}} = 2.57 \mu_{\text{B}}$ provides the number of unpaired electrons and corresponds to effective local magnetic moment μ_{eff} of $3.417 \mu_{\text{B}}$ and $3.430 \mu_{\text{B}}$, respectively. We obtain μ_{eff} values by:

$$\mu_{\text{eff}} = 2\sqrt{S(S+1)} \quad (5)$$

where S is the spin which equals to $\frac{1}{2} \times$ unpaired electron. In this case, the value of μ_{Co} is in fair agreement with that of the IS state ($t_{2g}^4 e_g^1, S = 3/2$) at Co^{4+} ion in which there are three unpaired electrons. Each electron approximately gives $1 \mu_{\text{B}}$. It is, thus, suggested that there is a possibility of mixing between IS states and a small number of LS states, which produces lower μ_{Co} rather than the theoretically predicted μ_{Co} , as shown in Table 4. Table 4 presents the possible valence states of Co ion, i.e. LS, IS, and HS.

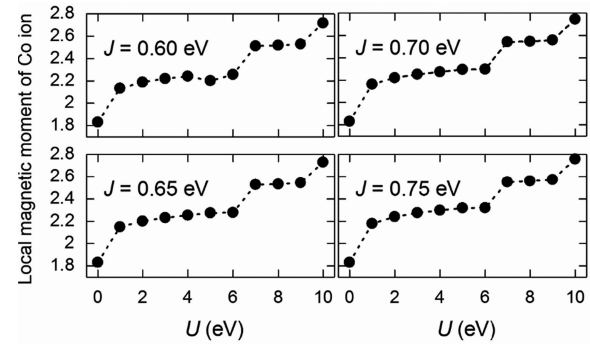


Fig. 3. Calculated local magnetic moments of Co ion as function of U for selected values of J in $\text{Pm}\bar{3}\text{m}$ space group.

It is concluded that the values of $U = 8 \text{ eV}$ or 9 eV ($J = 0.75 \text{ eV}$) are suitable. They are consistent with that of the previously suggested values of $(U, J) = (10.0 \text{ eV}, 0.76 \text{ eV})$ [10]. However, the value of $U = 8 \text{ eV}$ is in a very good agreement with that of previous reported values of $U = 7.8 \text{ eV}$ [40] and 8.0 eV [14]. The J-dependence of a, and μ_{Co} does not cause any significant change. According to these results, we then applied the value of $J = 0.75 \text{ eV}$, which is close to the previously reported J [13, 14, 40]. The analysis of both U values is further conducted by considering electronic and magnetic properties of the SrCoO_3 .

Regarding electronic and magnetic properties of SrCoO_3 , calculated projected-density of states (PDOS) of Co 3d orbitals, i.e. three-fold degenerate t_{2g} and two-fold degenerate e_g and O 2p states, for $U = 0 \text{ eV}$ to 10 eV and $J = 0.75 \text{ eV}$, are shown in Fig. 4. However, Sr 5s orbital provides almost no contribution to chemical bondings and

Table 2. Experimental results for lattice parameter, total and local magnetic moments, with corresponding measurement method and material type of SrCoO₃.

a [Å]	μ [μ _B /f.u]	T [K]	μ _{Co} [μ _B]	Measurement method	Material type	Literature
3.8289	2.5	2	–	SQUID magnetometer	Single crystal	[9]
3.8292	2.5	1.8	–	SQUID magnetometer	Polycrystalline	[45]
3.835	2.1	0 K	–	Foner-type magnetometer	Polycrystalline	[46]
3.836			3.0	Automatic recording balance	Crystal	[44]

Table 3. The values of lattice parameters, total and local magnetic moments, of SrCoO₃ obtained using theoretical studies.

Space group	a [Å]	c [Å]	μ [μ _B /f.u]	μ _{Co} [μ _B]	Temp. [K]	Literature
Pm $\bar{3}$ m	–	–	–	3.19	300 K	[14]
Pm $\bar{3}$ m	3.84	–	–	1.30	300 K	[10]
Pm $\bar{3}$ m	3.833	–	2.281	–	–	[15]
Pm $\bar{3}$ m	3.842	–	2.6	–	–	[5]
Pm $\bar{3}$ m	–	–	–	2.96 (IS)	–	[16]
Pm $\bar{3}$ m	–	–	–	2.70	232 K	[13]
P4/mbm (GGA + U)	3.943	5.502	–	2.84	0 K	[2]
P4/mbm (LDA + U)	3.811	5.313	–	2.86	0 K	[2]
P4/mbm (HSE06)*	3.912	5.429	–	2.53	0 K	[2]

*Hybrid-functional method: Heyd-Scuseria-Ernzerhof [47, 48].

phenomena around E_F . This is confirmed by the absence of electron in the outer shell of Sr²⁺ ion, described as [Kr]5s⁰ configuration. The ferromagnetic behavior is reflected by PDOS for all U values and it is mainly contributed by Co 3d states hybridized with O 2p states. We also suggest that the SrCoO₃ has metallic character, as reported in the previous reports [9, 15], which is summarized in Table 2 and Table 3. We thus propose that the values of U = 8 eV and J = 0.75 eV are the best values for SrCoO₃ with Pm $\bar{3}$ m space group. The calculated total energy per Co is –243.138 Ry (–3308 eV). Yet, IS state is also proposed in half-metallic SrCoO₃ studied by using the unrestricted Hartree-Fock (UHF) approximation, as shown in Table 3 [16].

Fig. 4 shows crystal-field effect in cubic symmetry, which produces three-degenerate Co 3d-t_{2g} and two-degenerate Co 3d-e_g states. The spin-up Co 3d-t_{2g} and Co 3d-e_g states are shifted to the lower energy and the spin-down states are shifted

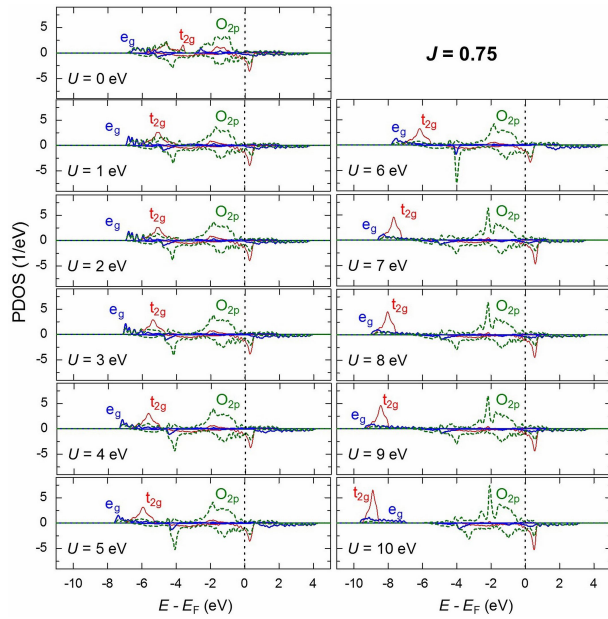
to the higher energy by increasing U. These shifts are suggested to be the result of suppression by the high U.

However, the Co 3d-t_{2g} states are much more sensitive to the change in U in the range of 6 eV ≤ U ≤ 7 eV. The enhanced sensitivity was described by the previous report showing similar sensitivities of Co 3d-t_{2g} and Co 3d-e_g states in the whole U range [14]. The spin-down t_{2g} states generally overlap the spin-down Co 3d-e_g states above E_F. On the other hand, for U ≤ 9 eV, smeared Co 3d-e_g and spin-up Co 3d-t_{2g} states are below E_F due to the hybridization with O 2p states. These results are similar to those of previous results [13, 15] but are different from the picture of IS-state t_{2g} [49]. However, the configuration of t_{2g}⁴e_g¹ in IS-state is reproduced by our calculations.

On the other hand, the spin-up O 2p states are quite strongly affected by increased U. Spin-up and spin-down O 2p peaks at around –2 eV (for U ≥ 7 eV) and –4 eV are O 2p_σ peaks

Table 4. Possible valence states and spin states with corresponding electron configurations and effective magnetic moment values calculated from equation 5.

Co valence state	LS		IS		HS	
	unpaired electron	$\mu_{\text{eff}} [\mu_B]$	unpaired electron	$\mu_{\text{eff}} [\mu_B]$	unpaired electron	$\mu_{\text{eff}} [\mu_B]$
2+	1 ($t_{2g}^6 e_g^1$)	1.732	—	—	3 ($t_{2g}^5 e_g^2$)	3.872
3+	0 ($t_{2g}^6 e_g^0$)	0	2 ($t_{2g}^5 e_g^1$)	2.828	4 ($t_{2g}^4 e_g^2$)	4.899
4+	1 ($t_{2g}^5 e_g^0$)	1.732	3 ($t_{2g}^4 e_g^1$)	3.872	5 ($t_{2g}^3 e_g^2$)	5.916

Fig. 4. Calculated projected-density of states of SrCoO₃ in Pm $\bar{3}$ m space group for U = 0 eV to 10 eV with J = 0.75 eV. The Fermi level is set to be zero as reference.

based on previously calculated PDOS by dynamical mean-field theory (DMFT) [13]. However, O 2p $_{\pi}$ states are not significantly changed. It is thus clear that U widens the separation between spin-up O 2p $_{\sigma}$ and O 2p $_{\pi}$ states. In addition, the hybridization of Co 3d-t $_{2g}$ and O 2p states is weakened by the increasing of U, while U-dependence of hybridization of Co 3d-e $_{g}$ and O 2p states is small. In spite of the presence of crystal-field effect in d orbitals, Jahn-Teller (JT) distortion has not been found for all U and J values. The spin-up and spin-down Co 3d-t $_{2g}$ states are evidently higher than the

Co 3d-e $_{g}$ states for U = 8 eV and J = 0.75 eV. Looking back, the proposed IS-LS states for both values of U and J as well as the local magnetic moment of Co ion are mainly contributed by spin-up t $_{2g}$ states at around -8.02 eV and spin-down t $_{2g}$ states at around 0.54 eV as shown in Fig. 4.

3.2. Bulk SrCoO₃ in P4/mbm space group

In this space group, J is not varied because J would not significantly change lattice parameters and local magnetic moment of Co ion as it has been found for the previous space group. Although U = 10 eV results in an overestimated value for the cubic symmetry, we used U = 0 eV to U = 10 eV to study the properties of SrCoO₃ in P4/mbm space group. The calculated tetragonal lattice parameters and their dependence on U for J = 0.75 eV are shown in Fig. 5. It is seen that the optimized a' (= $\sqrt{2}c$) and c are generally increased with increasing value of U. However, a' is minimum at U = 4 eV (5.4480 Å) and maximum at U = 10 eV (5.4809 Å). On the other hand, c is minimum at U = 3 eV (3.8489 Å) and maximum at U = 9 eV (3.9209 Å).

The values of U = 0 eV and U = 3 eV provide a good agreement with the results of the previous reports, presented in Table 2. The lattice parameters are however overestimated for U \geq 4 eV. The inset in Fig. 5 presents U-dependence of μ_{Co} . There is an increase in μ_{Co} from U = 0 eV to U = 1 eV and until U = 8 eV μ_{Co} remains nearly constant from 2.2431 μ_B to 2.3146 μ_B , which is close to the picture of IS states mixed with a few LS states for Co⁴⁺. The values of μ_{Co} are consistent with that obtained by using HSE06 method [2]. The values

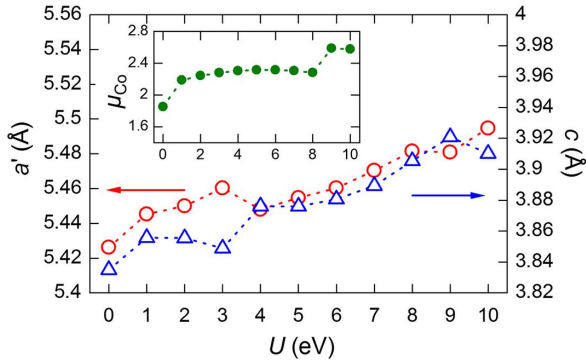


Fig. 5. Calculated tetragonal lattice parameters and local magnetic moments (μ_{Co}) of Co ion as function of U ($J = 0.75$ eV) in P4/mbm space group.

of $U = 9$ eV and 10 eV, respectively, give higher μ_{Co} values of 2.5871 eV and 2.5767 eV, which are close to the picture of IS states mixed with a few LS states for Co^{4+} as well. However, the overestimated tetragonal lattice parameters do not fit with the presented experimental reports, as shown in Table 2 and Table 3, although HSE06 also promotes the overestimated results [2]. Considering these results, we propose that $U = 3$ eV ($J = 0.75$ eV) is the most suitable for SrCoO_3 in P4/mbm space group. The calculated total energy per Co is -243.385 Ry (-3311 eV). It means P4/mbm space group results in more stable ground state rather than that of $\text{Pm}\bar{3}\text{m}$ after choosing the suitable U . Further analysis has been extended by the calculated electronic and magnetic properties.

The calculated PDOS of Co 3d orbitals, i.e., t_{2g} and e_g , and O 2p states for $U = 0$ eV to 10 eV at $J = 0.75$ eV for P4/mbm space group are shown in Fig. 6. As results for SrCoO_3 in $\text{Pm}\bar{3}\text{m}$ space group, PDOS of Sr^{2+} ion provides negligible contribution near E_F . Also, FM metallic behavior is found for this system in P4/mbm space group for all U values. Crystal-field effect is also found in this symmetry. The spin-up Co 3d states are shifted to the lower energy and the spin-down states are shifted to the higher energy with increasing U but the increase is not as significant as that of the system in $\text{Pm}\bar{3}\text{m}$ space group. Hence, it is suggested that the suppression of U to Co 3d binding energy levels is not as strong as in $\text{Pm}\bar{3}\text{m}$ space group. Until $U = 8$ eV, Co 3d- t_{2g} states are sensitive to

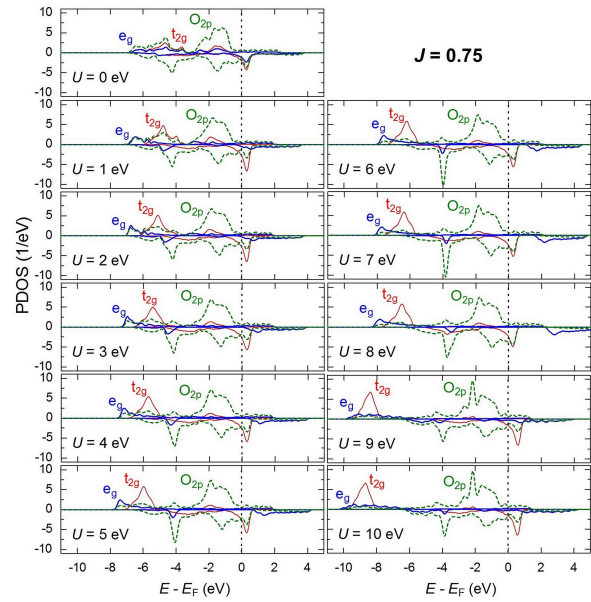


Fig. 6. Calculated projected-density of states of SrCoO_3 in P4/mbm space group for $U = 0$ eV to 10 eV with $J = 0.75$ eV. The Fermi level is set to be zero as reference.

changing of U in $5 \text{ eV} \leq U \leq 6 \text{ eV}$ range, while Co 3d- e_g states are not sensitive. For $U = 9$ eV and 10 eV, the profile of Co 3d states changes significantly and corresponds to high μ_{Co} . As also seen for $\text{Pm}\bar{3}\text{m}$ space group, the spin-down Co 3d- t_{2g} states overlap the spin-down Co 3d- e_g states above E_F . These results are also similar to the previously reported [13, 15] but are different from the picture of IS-state Co 3d- t_{2g} [49]. Interestingly, $t_{2g}^4 e_g^1$ configuration is also reproduced with P4/mbm space group. The spin-up O 2p states are strongly affected by the increasing U , especially in the range of $6 \text{ eV} \leq U \leq 7 \text{ eV}$. Spin-up and spin-down O 2p peaks at around -2 eV ($U = 9$ eV and 10 eV) and -4 eV are O $2p_\sigma$ peaks, which are strongly affected by U , based on previously calculated PDOS by DMFT [13]. It is also suggested that U widens the separation between spin-up O $2p_\sigma$ and O $2p_\pi$ states.

3.3. Norm-conserving pseudopotential for SrCoO_3

PDOS of SrCoO_3 obtained by using NC-PP, are shown in Fig. 7a. We found that the optimized a of

3.83 Å is in good agreement with experimental result [9] but the calculated μ_{Co} of $2.5267 \mu_{\text{B}}$ is lower than that of the picture of IS-state. The calculated total energy per Co is -151.965 Ry (-2680 eV), which is too high compared with that of US-PP. Furthermore, we found a sharp spin-down O 2p peak at -4.4 eV which is similar to the peak at -4.0 eV for $U = 6 \text{ eV}$ ($J = 0.75 \text{ eV}$) as shown in Fig. 7b. On the other hand, the separated spin-up O $2p_{\sigma}$ and O $2p_{\pi}$ peaks at -2.1 eV and around -1.2 eV for NC-PP are similar to the separated peaks at -2.18 and around -1.5 eV for $U = 8 \text{ eV}$ ($J = 0.75 \text{ eV}$) shown in Fig. 7c. The Co $3d-e_g$ and spin-up Co $3d-t_{2g}$ states for NC-PP also spread below E_{F} , while spin-down Co $3d-t_{2g}$ states lie above E_{F} and are hybridized with some spin-down O 2p states. Consequently, the employed NC-PP and US-PP with suitable U can be used to describe the electronic and magnetic properties of SrCoO_3 in $\text{Pm}\bar{3}\text{m}$ space group.

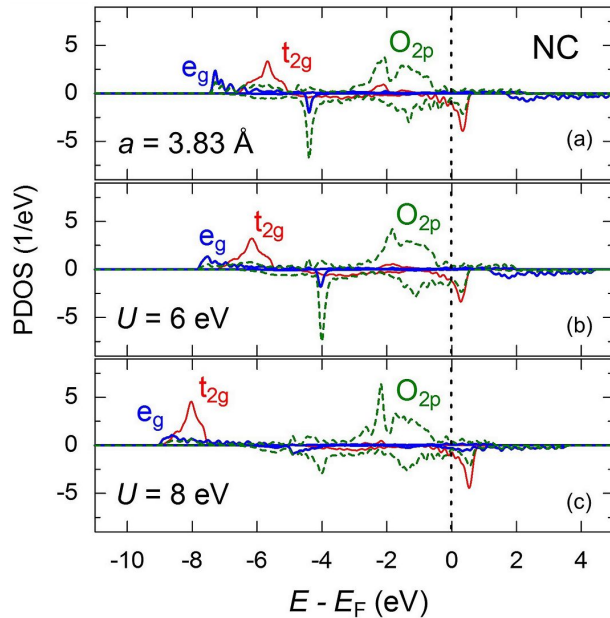


Fig. 7. Calculated projected-density of states of d and O 2p orbitals in SrCoO_3 in $\text{Pm}\bar{3}\text{m}$ space group (a) for norm-conserving pseudopotential, (b) $U = 6 \text{ eV}$, (c) $U = 8 \text{ eV}$.

PDOS of SrCoO_3 in $\text{P4}/\text{mbm}$ space group obtained by using NC-PP is shown in Fig. 8a. We found that c of 3.884 Å is overestimated

relative to the experiments (Table 2). The calculated μ_{Co} of $2.5953 \mu_{\text{B}}$ is lower than that of the picture of IS-state.

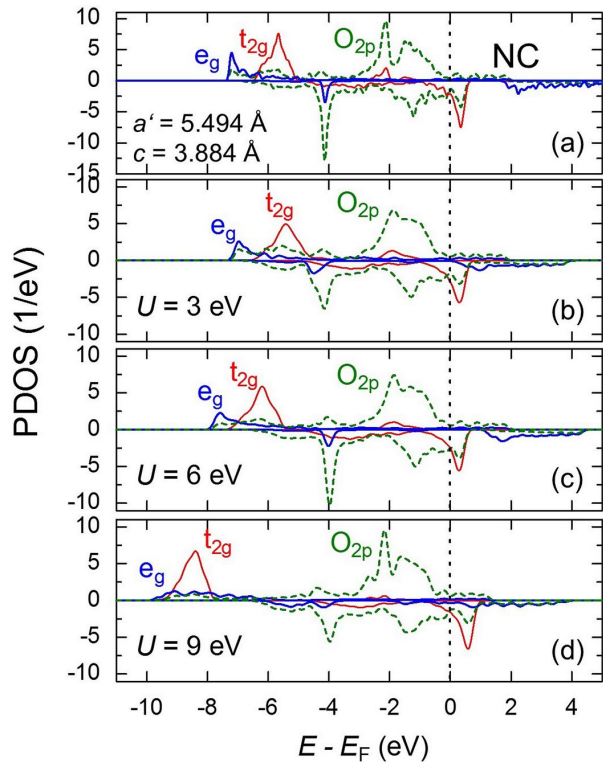


Fig. 8. Calculated projected-density of states of d and O 2p orbitals in SrCoO_3 in $\text{P4}/\text{mbm}$ space group (a) for norm-conserving pseudopotential, (b) $U = 3 \text{ eV}$, (c) $U = 6 \text{ eV}$.

Calculated total energy per Co is -303.930 Ry (-4135 eV), which is lower than that of US-PP. We have also found a sharp spin-down O 2p peak at -4.2 eV which is similar to the peak at -4.0 eV for $U = 6 \text{ eV}$ ($J = 0.75 \text{ eV}$) as shown in Fig. 8c. On the other hand, separated spin-up O $2p_{\sigma}$ and O $2p_{\pi}$ peaks at -2.1 eV and around -1.3 eV for NC-PP are close to the separated peaks at -2.18 and around -1.5 eV for $U = 9 \text{ eV}$ ($J = 0.75 \text{ eV}$) shown in Fig. 8d. The Co $3d-e_g$ and spin-up Co $3d-t_{2g}$ states for NC-PP also spread below the E_{F} , while spin-down Co $3d-t_{2g}$ states lie above E_{F} and are hybridized with some spin-down O 2p states. However, the PDOS profile for NC-PP is different from that for $U = 3 \text{ eV}$, as shown in Fig. 8b. We can conclude that US-PP with GGA + U method is

more suitable for SrCoO₃ in P4/mbm space group rather than NC-PP with GGA method, in spite of the lower ground-state total energy.

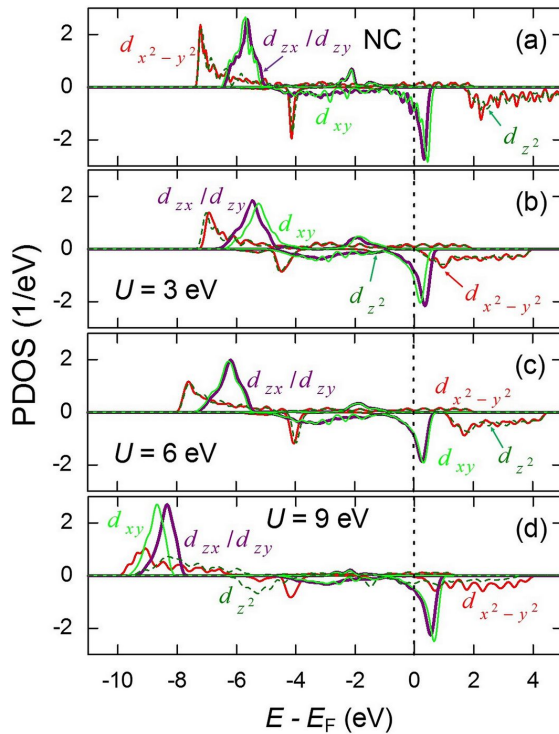


Fig. 9. Calculated projected-density of states of d in SrCoO₃ in P4/mbm space group (a) for normal-conserving pseudopotential, (b) $U = 3$ eV, (c) $U = 6$ eV, and (d) $U = 9$ eV.

Interestingly, JT distortion is found in P4/mbm space group. Fig. 9a shows JT distortion in Co 3d orbital obtained by using NC-PP. It is found that the spin-up Co 3d_{xy} level is below Co 3d_{zx}/Co 3d_{zy} levels, while the spin-down Co 3d_{xy} level is at the highest level. The spin-up and spin-down Co 3d_{z₂} levels are close to Co 3d_{x²-y²} level. This profile is very similar to that for $U = 6$ eV, as shown in Fig. 9c. For $U = 3$ eV, this profile is different from that calculated using NC-PP. The spin-up Co 3d_{xy} level is above Co 3d_{zx}/Co 3d_{zy} levels, while the spin-down Co 3d_{xy} level is at the lowest level, as shown in Fig. 9b. Interestingly, a large JT distortion is found for $U = 9$ eV in which the spin-up Co 3d_{xy} level is below Co 3d_{zx}/Co 3d_{zy} levels and the spin-down Co 3d_{xy} level is at the highest level, as shown in Fig. 9d. This also applies to

Co 3d-e_g in which spin-up Co 3d_{z₂} level is higher than Co 3d_{x²-y²} level and spin-down Co 3d_{z₂} level is approximately the same as Co 3d_{x²-y²} level, especially above E_F . This result remarkably shows the significance of U contribution to JT distortion in Co 3d in P4/mbm space group, in contrast with that in Pm $\bar{3}$ m space group. The increasing of U strongly flips each d orbital in t_{2g}.

4. Conclusions

Based on the analysis, the values of $U = 8$ eV and $J = 0.75$ eV are the best choice for the SrCoO₃ description in terms of the local magnetic moment of Co ion and electronic structure for Pm $\bar{3}$ m space group. We found that the Co ion has a local magnetic moment of 2.56 μ_B , which is in good agreement with the previous results obtained by theoretical (3.19 μ_B) and experimental (3.0 μ_B) studies. The resulted PDOS shows that the Co 3d states are the main contributor to FM metallic properties of SrCoO₃, alongside with their hybridization with O 2p states. Otherwise, the Sr 5s states do not play almost any role. In general, increasing of U causes the shift of spin-up and spin-down Co 3d states to lower energy and higher energy, respectively. We also confirm that NC-PP calculation gives the lattice parameter which is in good agreement with experimental result, while Co ion local magnetic moment is still too low compared with the picture of IS-state. However, NC-PP is not suitable to be used for P4/mbm space group. The value of $U = 3$ eV ($J = 0.75$) is the most suitable choice for this space group. For this U value, FM metallic properties and good agreement of tetragonal lattice parameters with experimental results are also obtained but the local magnetic moment of Co ion is much lower than the picture of IS state. This indicates that LS states for P4/mbm space group have larger contribution to Co 3d orbital rather than that for Pm $\bar{3}$ m space group. Interestingly, the result also shows the significance of U contribution to JT distortion in Co 3d for P4/mbm space group even though the shifts of each orbitals are consistent with that for Pm $\bar{3}$ m space group. This study generally shows the significant contribution of U and space group in calculating

structural, electronic, and magnetic properties of SrCoO₃. Based on the more stable ground state, it also shows that P4/mbm space group with US-PP is more suitable for connecting the theoretical and observed experimental properties after choosing the suitable U value.

Acknowledgements

The authors acknowledge Prof. May O. Tjia for fruitful discussion on theoretical understanding in this paper. The authors also acknowledge the Advanced Computing Laboratory, Department of Physics, Institut Teknologi Bandung, Indonesia, for providing computation facilities and technical supports.

References

- [1] VERMA A., RAGHAVAN S., STEMMER S., JENA D., *Appl. Phys. Lett.*, 107 (2015), 192908.
- [2] RIVERO P., CAZORLA C., *Phys. Chem. Chem. Phys.*, 18 (2016), 30686.
- [3] KAMBA S., GOIAN V., SKOROMETS V., HEJTMÁNEK J., BOVTUN V., KEMPA M., BORODAVKA F., VANĚK P., BELIK A., LEE J., *Phys. Rev. B*, 89 (2014), 064308.
- [4] SUSHRISANGITA S., MAHAPATRA P.K., CHOUDHARY R.N.P., *J. Physics D Appl. Phys.*, 49 (2016), 035302.
- [5] LEE J.H., RABE K.M., *Phys. Rev. Lett.*, 107 (2011), 067601.
- [6] SEÑARÍS-RODRÍGUEZ M.A., GOODENOUGH J.B., *J. Solid State Chem.*, 116 (1995), 224.
- [7] UCHIDA H., ARISAKA S., WATANABE M., *Solid State Ion.*, 135 (2000), 347.
- [8] SUTJAHJA I., BERTHALITA F., MUSTAQIMA M., NUGROHO A., TJIA M., *Mater. Sci.-Poland*, 33 (2015), 579.
- [9] LONG Y., KANEKO Y., ISHIWATA S., TAGUCHI Y., TOKURA Y., *J. Phys. Condens. Mat.*, 23 (2011), 245601.
- [10] HAI-PING W., KAI-MING D., FENG-LAN H., WEI-SHI T., CHUN-MEI T., QUN-XIANG L., *Chin. Phys. Lett.*, 26 (2009), 017105.
- [11] NEMUDRY A., RUDOLF P., SCHÖLLHORN R., *Chem. Mater.*, 8 (1996), 2232.
- [12] JAYA S.M., JAGADISH R., RAO R., ASOKAMANI R., *Phys. Rev. B*, 43 (1991), 13274.
- [13] KUNEŠ J., KRÁPEK V., PARRAGH N., SANGIOVANNI G., TOSCHI A., KOZHEVNIKOV A., *Phys. Rev. Lett.*, 109 (2012), 117206.
- [14] HAI-PING W., DONG-GUO C., DE-CAI H., KAI-MING D., *Acta Phys. Sin.*, 61 (2012), 037101.
- [15] HOFFMANN M., BORISOV V.S., OSTANIN S., MERTIG I., HERGERT W., ERNST A., *Phys. Rev. B*, 92 (2015), 094427.
- [16] ZHUANG M., ZHANG W., HU A., MING N., *Phys. Rev. B*, 57 (1998), 13655.
- [17] KOTLIAR G., SAVRASOV S.Y., HAULE K., OUDOVENKO V.S., PARCOLLET O., MARIANETTI C., *Rev. Mod. Phys.*, 78 (2006), 865.
- [18] MAVROPOULOS P., PAPANIKOLAOU N., *The Kohn-Rostoker (KKR) Green Function Method I. Electronic Structure of Periodic Systems*, in: GROTE-DORST J., BLÜGEL S., MARX D. (Eds.), *Computational Nanoscience: Do It Yourself!*, John von Neumann Institute for Computing, Jülich, 2006. p. 131.
- [19] AMOS T., SNYDER L.C., *J. Chem. Phys.*, 41 (1964), 1773.
- [20] RAD A.S., KASHANI O.R., *Appl. Surf. Sci.*, 355 (2015), 233.
- [21] ATANASOV M., ARAVENA D., SUTURINA E., BILL E., MAGANAS D., NEESE F., *Coord. Chem. Rev.*, 289 – 290 (2015), 177.
- [22] YANG J., HU W., USVYAT D., MATTHEWS D., SCHÜTZ M., CHAN G.K.-L., *Science*, 345 (2014), 640.
- [23] MUHAMMADY S., KURNIAWAN R., NURFANI E., SUTJAHJA I.M., WINATA T., DARMA Y., *J. Phys. Conf. Ser.*, 776 (2016), 012018.
- [24] MUHAMMADY S., NURFANI E., KURNIAWAN R., SUTJAHJA I.M., WINATA T., DARMA Y., *Mater. Res. Express*, 4 (2017), 024002.
- [25] WANG Y., MA J., ZHOU J.-P., CHEN X.-M., WANG J.-Z., *J. Korean Phys. Soc.*, 68 (2016), 409.
- [26] PERDEW J.P., BURKE K., ERNZERHOF M., *Phys. Rev. Lett.*, 77 (1996), 3865.
- [27] GIANNOZZI P., BARONI S., BONINI N., CALANDRA M., CAR R., CAVAZZONI C., CERESOLI D., CHIAROTTI G.L., COCCIONI M., DABO I., CORSO A.D., GIRONCOLI S.D., FABRIS S., FRATESI G., GEBAUER R., GERSTMANN U., GOUGOUSSIS C., KOKALJ A., LAZZERI M., MARTIN-SAMOS L., MARZARI N., MAURI F., MAZZARELLO R., PAOLINI S., PASQUARELLO A., PAULATTO L., SBRACCIA C., SCANDOLO S., SCLAUZERO G., SEITSONEN A.P., SMOGUNOV A., UMARI P., WENTZCOVITCH R.M., *J. Phys. Condens. Mat.*, 21 (2009), 395502.
- [28] HOHENBERG P., KOHN W., *Phys. Rev.*, 136 (1964), B 864.
- [29] KOHN W., SHAM L.J., *Phys. Rev.*, 140 (1965), A 1133.
- [30] BROYDEN C.G., *Math. Comp.*, 19 (1965), 577.
- [31] RAPPE A.M., RABE K.M., KAXIRAS E., JOANNOPOULOS J., *Phys. Rev. B*, 41 (1990), 1227.
- [32] VANDERBILT D., *Phys. Rev. B*, 41 (1990), 7892.
- [33] BROYDEN C.G., *IMA J. Appl. Math.*, 6 (1970), 76.
- [34] FLETCHER R., *Comput. J.*, 13 (1970), 317.
- [35] GOLDFARB D., *Math. Comp.*, 24 (1970), 23.
- [36] SHANNO D.F., *Math. Comp.*, 24 (1970), 647.
- [37] LOUIE S.G., FROYEN S., COHEN M.L., *Phys. Rev. B*, 26 (1982), 1738.
- [38] REIS C.L., PACHECO J., MARTINS J.L., *Phys. Rev. B*, 68 (2003), 155111.
- [39] COCCIONI M., GIRONCOLI DE S., *Phys. Rev. B*, 71 (2005), 035105.
- [40] ANISIMOV V.I., ZAAANEN J., ANDERSEN O.K., *Phys. Rev. B*, 44 (1991), 943.

- [41] TROULLIER N., MARTINS J.L., *Solid State Commun.*, 74 (1990), 613.
- [42] TROULLIER N., MARTINS J.L., *Phys. Rev. B*, 43 (1991), 1993.
- [43] TROULLIER N., MARTINS J.L., *Phys. Rev. B*, 43 (1991), 8861.
- [44] TAGUCHI H., SHIMADA M., KOIZUMI M., *Mater. Res. Bull.*, 13 (1978), 1225.
- [45] BALAMURUGAN S., TAKAYAMA-MUROMACHI E., *J. Solid State Chem.*, 179 (2006), 2231.
- [46] BEZDICKA P., WATTIAUX A., GRENIER J., POUCHARD M., HAGENMULLER P., *Z. Anorg. Allg. Chem.*, 619 (1993), 7.
- [47] HEYD J., SCUSERIA G.E., ERNZERHOF M., *J. Chem. Phys.*, 118 (2003), 8207.
- [48] HEYD J., SCUSERIA G.E., ERNZERHOF M., *J. Chem. Phys.*, 124 (2006), 219906.
- [49] POTZE R., SAWATZKY G., ABBATE M., *Phys. Rev. B*, 51 (1995), 11501.

Received 2017-05-24

Accepted 2017-10-05